REPORT DOCUMENTATION PAGE

Form Approved OMB NO. 0704-0188

1. REPORT DATE (DD-MM-YYYY)	2. REPORT TYPE	3. DATES COVERED (From - To)
27-04-2015	Final Report	1-May-2009 - 31-Dec-2014

4. TITLE AND SUBTITLE
Final Report: Nanopatterned Quantum Dot Lasers for High Speed, High Efficiency, Operation

5a. CONTRACT NUMBER
W911NF-09-1-0127

5b. GRANT NUMBER

5c. PROGRAM ELEMENT NUMBER
611102

6. AUTHORS
Luke Mawst

5d. PROJECT NUMBER

5e. TASK NUMBER

5f. WORK UNIT NUMBER

7. PERFORMING ORGANIZATION NAMES AND ADDRESSES
University of Wisconsin - Madison
RESERACH & SPONSORED PROGRAMS
21 N. PARK STREET SUITE 6401
MADISON, WI 53715 -1218

8. PERFORMING ORGANIZATION REPORT NUMBER

9. SPONSORING/MONITORING AGENCY NAME(S) AND ADDRESS (ES)
U.S. Army Research Office
P.O. Box 12211
Research Triangle Park, NC 27709-2211

10. SPONSOR/MONITOR'S ACRONYM(S)
ARO

11. SPONSOR/MONITOR'S REPORT NUMBER(S)
55888-EL.8

12. DISTRIBUTION AVAILIBILITY STATEMENT
Approved for Public Release; Distribution Unlimited

13. SUPPLEMENTARY NOTES
The views, opinions and/or findings contained in this report are those of the author(s) and should not contrued as an official Department of the Army position, policy or decision, unless so designated by other documentation.

14. ABSTRACT
Quantum dot (QD) active regions hold potential for realizing extremely high performance semiconductor diode lasers. Unfortunately, these unique features of ideal QD active layers have not been fully realized to date. The most successful approach to date of forming QD's is self-assembly under the Stranski–Krastanow (SK) growth mode. However, this approach results in a relatively large distribution of QD sizes, leading to significant inhomogeneous broadening of the spectral gain. SK QDs inherently form on top of a two-dimensional "wetting layer", leading to weak electron and hole confinement to the QD, which results in low gain saturation. Here, we have investigated the

15. SUBJECT TERMS
quantum dots, nanopatterning, MOCVD, laser

16. SECURITY CLASSIFICATION OF:			17. LIMITATION OF ABSTRACT	15. NUMBER OF PAGES	19a. NAME OF RESPONSIBLE PERSON
a. REPORT	b. ABSTRACT	c. THIS PAGE			Luke Mawst
UU	UU	UU	UU		19b. TELEPHONE NUMBER 608-263-1705

Report Title

Final Report: Nanopatterned Quantum Dot Lasers for High Speed, High Efficiency, Operation

ABSTRACT

Quantum dot (QD) active regions hold potential for realizing extremely high performance semiconductor diode lasers. Unfortunately, these unique features of ideal QD active layers have not been fully realized to date. The most successful approach to date of forming QD's is self-assembly under the Stranski–Krastanow (SK) growth mode. However, this approach results in a relatively large distribution of QD sizes, leading to significant inhomogeneous broadening of the spectral gain. SK QDs inherently form on top of a two-dimensional "wetting layer", leading to weak electron and hole confinement to the QD, which results in low gain saturation. Here, we have investigated the use of dense nanoscale diblock copolymer lithography-based nanofabrication and selective quantum dot growth using metalorganic chemical vapor deposition (MOCVD). These methods allowed us to realize quantum dot active regions in which the injected carriers exhibit full three-dimensional nano-scale confinement and elimination of the wetting layer states. The objectives of this project were to develop lasers employing the nano-patterned QD active regions and investigate the characteristics of these novel active regions

---

Enter List of papers submitted or published that acknowledge ARO support from the start of the project to the date of this printing. List the papers, including journal references, in the following categories:

(a) Papers published in peer-reviewed journals (N/A for none)

Received Paper

TOTAL:

Number of Papers published in peer-reviewed journals:

(b) Papers published in non-peer-reviewed journals (N/A for none)

Received Paper

TOTAL:

Number of Papers published in non peer-reviewed journals:

(c) Presentations

Number of Presentations: 0.00

Non Peer-Reviewed Conference Proceeding publications (other than abstracts):

Received		Paper
08/22/2011	3.00	Y. Huang, J. Kirch, L. J. Mawst, Y. Sin, J. H. Park, B. Foran, C.-C. Liu, P. F. Nealey, T. F. Kuech. Nanopatterned quantum dot active region lasers on InP substrates, Novel In-Plane Semiconductor Lasers X. 23-JAN-11, San Francisco, California, USA. : ,
TOTAL:	**1**	

Number of Non Peer-Reviewed Conference Proceeding publications (other than abstracts):

Peer-Reviewed Conference Proceeding publications (other than abstracts):

Received		Paper
08/22/2011	4.00	J. H. Park, Y. Huang, J. Kirch, T. Kim, C.-C. Liu, P. F. Nealey, T. F. Kuech, Y. Sin, B. Foran, L. J. Mawst. Quantum dot active regions based on diblock copolymer nanopatterning and selective MOCVD growth, 2011 IEEE Winter Topicals (WTM). 09-JAN-11, Keystone, CO, USA. : ,
08/22/2011	6.00	T. F. Kuech, L. J. Mawst. Patterned InGaAs/InGaAsP/InP quantum dot active lasers using diblock copolymer lithography and selective area MOCVD growth, 2010 23rd Annual Meeting of the IEEE Photonics Society (Formerly LEOS Annual Meeting). 06-NOV-10, Denver, CO, USA. : ,
08/29/2012	7.00	Y. Huang , T. Kim, T. Garrod, L. J. Mawst, S. Xiong, P. F. Nealey, K. Schulte, T. F. Kuech. Nanofabrication of Quantum Dots on InP by In-Situ Etching and Selective Growth, IEEE CLEO 2012. 06-MAY-12, . : ,
TOTAL:	**3**	

Number of Peer-Reviewed Conference Proceeding publications (other than abstracts):

(d) Manuscripts

Received Paper

TOTAL:

Number of Manuscripts:

Books

Received Book

TOTAL:

Received Book Chapter

TOTAL:

Patents Submitted

Patents Awarded

Awards

IEEE Fellow 2012

Graduate Students

NAME	PERCENT_SUPPORTED	Discipline
Honghyuk Kim	0.33	
Yinggang Huang	0.33	
Joo Park	0.33	
FTE Equivalent:	**0.99**	
Total Number:	**3**	

Names of Post Doctorates

NAME	PERCENT_SUPPORTED
FTE Equivalent:	
Total Number:	

Names of Faculty Supported

NAME	PERCENT_SUPPORTED	National Academy Member
Luke Mawst	0.10	
Thomas Kuech	0.10	Yes
FTE Equivalent:	**0.20**	
Total Number:	**2**	

Names of Under Graduate students supported

NAME	PERCENT_SUPPORTED
FTE Equivalent:	
Total Number:	

Student Metrics

This section only applies to graduating undergraduates supported by this agreement in this reporting period

The number of undergraduates funded by this agreement who graduated during this period: 0.00

The number of undergraduates funded by this agreement who graduated during this period with a degree in science, mathematics, engineering, or technology fields:..... 0.00

The number of undergraduates funded by your agreement who graduated during this period and will continue to pursue a graduate or Ph.D. degree in science, mathematics, engineering, or technology fields:..... 0.00

Number of graduating undergraduates who achieved a 3.5 GPA to 4.0 (4.0 max scale):..... 0.00

Number of graduating undergraduates funded by a DoD funded Center of Excellence grant for Education, Research and Engineering:..... 0.00

The number of undergraduates funded by your agreement who graduated during this period and intend to work for the Department of Defense 0.00

The number of undergraduates funded by your agreement who graduated during this period and will receive scholarships or fellowships for further studies in science, mathematics, engineering or technology fields:..... 0.00

Names of Personnel receiving masters degrees

NAME
Yinggang Huang
Total Number: **1**

Names of personnel receiving PHDs

NAME
Joo Park
Total Number: 1

Names of other research staff

NAME	PERCENT_SUPPORTED
FTE Equivalent:	
Total Number:	

Sub Contractors (DD882)

Inventions (DD882)

Scientific Progress

See attached file

Technology Transfer

Throughout the program I have interacted closely with Dr. Yongkun Sin at The Aerospace Corporation. They have contributed with TEM measurements of the QDs fabricated in this program.

While Stranski-Krastnow (SK) growth mode self-assembled QDs on GaAs have enjoyed considerable success for device applications, such structures are less well developed on InP substrates. Often elongated structures (i.e. quantum dashes) are observed on InP instead of spherical shaped dots[1]. In addition, MOCVD grown SK QDs generally exhibit a bi-modal size distribution as well as the inherent wetting layer beneath the QD layer. The wetting layer has been identified as a path of leakage current which is an underlying cause for low optical gain and higher device temperature sensitivity, commonly observed in self-assembled QD lasers[2]. An alternate approach to SK QD formation is the use of nanopatterning with diblock copolymers combined with selective MOCVD growth, enabling QD formation over large surface areas intended for device application[3-5]. This approach allows for increased control over the QD size and distribution and elimination of the problematic wetting layer. High QD densities are achieved (>$6x10^{10}$ cm^2) with a process applicable to large surface coverage, showing promise for implementation into long wavelength (λ = 1.3-1.5μm) sources. In this project, we have demonstrated LT (up to 170K) InP-based laser operation from devices employing patterned QDs (~ 20 nm dia.). Prior reports of patterned QD active lasers on GaAs have shown promising results in terms of low threshold current densities[6], although little is known concerning InP-based patterned QD active lasers.

The diblock copolymer nanopatterning process consists of a series of pattern-transfers from a dense array of nano-sized holes in a diblock copolymer thin film to a dielectric template mask, allowing the patterned access to the InP substrate for selective growth of the QDs. SiN_x (10 nm) / InP(100) substrates were employed using the diblock copolymer process and selective MOCVD growth, as reported previously.[5,7] Fig. 1 shows a top view SEM image after the selective growth (610ºC) of InGaAsP Q1.15μm (2nm)/ $In_{0.53}Ga_{0.47}As$ (2nm)/InGaAsP Q1.15μm (2nm) QDs on top of the nanopatterned InGaAsP/n:InP waveguide/cladding layer, forming the bottom half of a device structure. A schematic diagram of the QD laser structure is shown in Fig. 2. We have reported on the RT PL emission from such structures in ref. 7. After QD growth, the dielectric mask is removed followed by the regrowth of the top InGaAsP Q1.15μm SCH waveguide region and p: InP cladding layer at 620ºC to complete the laser device structure. We found that the QD emission wavelength blueshifts by 200nm after the upper waveguide/cladding regrowth and laser oscillation is not observed[12]. However, by employing a lower temperature (550ºC) SCH and cladding layer regrowth to bury the QD active region, we have been able to largely suppress the blue shift. Ridge-waveguide lasers were then fabricated and the electroluminescence (EL) spectrum was measured at LT (20K), as shown in Fig. 3. Laser operation (J_{th}~1.9KA/cm^2 at 20K) is observed from devices with 50 μm–wide stripes and 3.6 mm-long cavities up to temperatures of 170K. Based on the shorter emission wavelength (~1.3 μm) observed here, compared with that of the LT PL spectral peak (~1.4 μm), it appears that lasing may occur on a higher energy (excited state) QD transition. Further improvements in QD growth and pre-etching are expected to lead to ground state emission with lower current densities. Multi-segmented devices have also been fabricated for amplified spontaneous emission (ASE) measurements to allow extraction of the optical spectral gain and overall radiative efficiency, which could provide further insights into the operation of these devices. However, since only low temperature operation was achieved, it was not possible to collect sufficient data from the multi-segmented devices.

Cross-sectional TEM studies, Fig. 4, of the nanopatterned QD active regions confirm full three-dimensional confinement through the absence of a wetting layer. Since the QD formation

does not rely on strain, as for self-assembled QDs, the strain of the $In_xGa_{1-x}As$ QDs can be varied over a large range from tensile-strain to compressive strain. Note that the composition of the $In_xGa_{1-x}As$ layers used in the QDs is determined from planar layer structures, so there is uncertainty in the actual composition within the QDs, due to the selective growth occurring only within the nano-sized openings of the dielectric mask. For the InAs QDs, the InAs layers were in the range of 1.5-2.5nm thick and surrounded by nominally lattice-matched InGaAs layers, as shown in Fig. 5. Low temperature photoluminescence measurements indicate that the emission wavelength of the QDs ranges from 1.4 μm for tensile-strained QDs to 2.1μm for compressively strained (InAs) QDs (Fig. 3). Shorter emission wavelengths are expected by implementing larger tensile strain, potentially accessing the 1.3 μm wavelength region. Longer emission wavelength into the mid-IR spectral region may be possible through the use of patterned formation of InAs QDs on materials with larger lattice constant, such as metamorphic buffers layers.

Optimization on dielectric mask and RIE condition for Multiple QD stacks

Park et al's demonstration in 1997 on BCP lithography opened a way to fabricate nano-sized uniform array in the absence of the wetting layer[8]. Also, *Li et al* showed that it is possible to fabricate periodic dense arrays of hole pattern can be achieved using cylinder-forming block copolymer with a high degree of pore-size uniformity through the pattern transfer procedures by the selective MOCVD growth[9].

As shown in Fig.6, when transferring the pattern onto the dielectric mask, reactive ion etching has been used other than wet etching in order to avoid its inherent undercutting and its heavy dependence on the location on the wafer, which potentially increase the chance of resulting in larger and non-uniform QD arrays. However, it was also observed that RIE creates significant amount of plasma damage on the surface of the sample, which will, in return, increase the number of non-radiative recombination centers on the surface. Therefore, in order to avoid both undercutting and the surface damage, it is necessary to have the minimum etching time as well as faster etching rate while this process has to be done in the controllable range of time. Also, the dielectric has to be completely removed selectively by wet etchant in a short time after the QD growth. Thus, to address these issues, the processes involving the dielectric mask deposition and RIE conditions were optimized.

Even though J. *Park et* al has successfully reported uniform and dense QD arrays employing dilock copolymer lithography, their photoluminescence at room temperature was relatively low[10]. To increase the PL intensity and optical gain, multiple stacks of QD grown by SK growth mode has been utilized[11]. However, unlike the case of SK growth mode, the number of stack is limited by the dielectric mask thickness for this selective growth. In this section, the optimization on dielectric and the following RIE is discussed to have thicker dielectric hard mask.

It is known that SiN_x is a significantly better diffusion and chemical barrier than SiO_x. Therefore, SiN_x deposited by PECVD has been chosen as a dielectric mask. Also, in order to achieve the faster etching rate in both HF-based solution and RIE using CF4 plasma, the flow rate ratio of NH_3

and SiH_4 was increased so that the resulting SiN_x is N-rich. It was checked that the etching rate of N-rich SiN_x is faster than Si-rich SiN_x under the same RIE condition, which agrees with the reports by *Williams et al* [12, 13]. Low r.f. power was also employed to increase the uniformity in the thickness.

r.f. Power	NH3/SiH4 ratio	Temperature	Deposition Rate
25W	6	250°C	0.054nm/s

<Table 1: Optimized PECVD SiNx parameters>

In order to prevent the polymer mask from being attacked during RIE, pure CF4 plasma was used to transfer the pattern onto the SiN_x hard mask. During this process, low pressure and gas flow were chosen so that the undercut of SiN_x is minimized. Also, the moderate amount of r.f. power was used to avoid the erosion of polymer and to result in shorter yet controllable etching time.

r.f. Power	Pressure	CF4 Gas flow
100W	10mTorr	10sccm

<Table 2: Optimized RIE parameters>

In order to have multiple stacks of QDs for higher luminescence and gain, it is desirable to have thicker SiN_x layers. Previously, we employed only about 10nm of SiN_x , resulting in uniform and dense single-stack QD arrays. Using the optimized recipes for SiN_x and RIE, it became possible to have uniform and dense QD arrays with thicker (20nm) SiN_x, with the etching time of 17 second. This thickness allowed us to achieve up to three-stack QD structure. Specific details will be discussed in the next section.

Stacked QD arrays as a gain medium for laser diode require them to be grown on the lower part of the separate confinement heterostructure(SCH) as shown in Fig 7. 1.5μm thick n: InP($5 \times 10^{17} cm^{-3}$) and 150nm thick InGaAsP($\lambda_g = 1.15\mu m$) lattice-matched to InP were grown at 630°C by MOCVD on the InP substrate as a laser base with precursors of TMIn, TMGa, AsH_3, and PH_3. Then, SiN_x was deposited for 460 second, using the optimized parameters. After 20nm thick SiN_x deposition, the sample was annealed in the MOCVD reactor under AsH_3 and PH_3 flow for 30 min at 630°C, as it was reported that annealing prevents SiN_x from being cracked during QD growth and improves the adhesion[10]. Then, 50nm thick cylinder-forming BCP was patterned on the laser base. In order to find the optimized RIE time, the pattern-transfer onto SiNx mask has been carried out by RIE for 17sec. After having wet treatment in diluted HCl and acetic acid to recover plasma damage for 30 sec, three stack InGaAs QD structures consisting of 3 x InGaAsP/InGaAs/InGaAsP (2nm each) was grown at 630°C. Right before the QD growth, *in-situ* etching targeting 2.5nm was done using CBr4 to remove the remaining plasma damage[14, 15]. After QD growth, the SiN_x hard mask was removed by 6:1 buffered oxide etchant (BOE) for 30 second.

To grow the uniform and homogeneous capping layer after the SiN_x removal, it is important to completely remove it for a short time using a wet etchant. Since both concentrated HF and phosphoric based acid attack InP-based semiconductor material, BOE was selected, which is known as an excellent selective etchant for SiNx. After SiN_x removal process, scanning electron microscopic images were taken to check the size of QD grown as well as SiN_x removal as shown in Fig. 4.

It can be clearly seen that with RIE time of 17 second, the pattern of the BCP was well transferred onto the SiN_x hard mask, and the subsequent growth resulted in the uniformly arrayed QDs with the diameter of ~33nm. To check the reproducibility, *this process has been repeated multiple times,* and the results remained the same, confirming its reproducibility. The density of QDs was found to be $\sim 6.1 \times 10^{10}\ \mathrm{cm}^{-2}$, which is comparable with J. *Park*'s result[10]. Also, it was confirmed that 6:1 BOE can selectively etch away SiN_x within 30sec.

Shown in Fig. 5 is a high-resolution transmission electron microscopic image of the cross section of a QD stack in the array. These image were obtained from our collaborators (Dr. Yongkun Sin) at The Aerospace Corporation. Fig. 5 (b) shows the periodic twinning plane developed during the QD growth, which were reported in the context of nanowire(NW) growth in the literature, originated from the coexistence of zinc blende(ZB) and wurtzite(WZ) crystal structure when grown epitaxially in a close-packed direction[16-19]. Fig. 6 shows a HR-STEM image of a QD stack in which, again, stacking faults are indicated. In reference 19, Shtrikman *et al* demonstrated employing highly terraced (311)B substrate resulted in stacking-faults-free zinc blende GaAs nanowires. Therefore, a similar approach may be employed in the future for the stacked QD materials. Also, for the better interface before the regrowth of QDs as well as subsequent capping layers, effectiveness of *in-situ* etching on InGaAsP and InP layer using CBr_4 will need to be verified and optimized.

Photoluminescence (PL) Study of Stacked QDs

The optical characteristics of QDs grown were investigated by PL measurement at various temperatures. The PL measurements were carried out using a continuous-wave Ar-ion pump laser at a wavelength of 514nm. The data was collected using a grating monochrometer and a cooled germanium detector. Low temperature measurements carried out with the sample mounted in a continuous-flow liquid-helium cryostat and cooled to 15K. Also, the capping layer was not grown on the QD layer. To observe the characteristics of the QDs, multiple quantum wells, which were grown without the patterning, were grown on the same laser base at the same condition as the growth of the stacked QDs.

Shown in Fig. 7 are PL spectra measured from 15K to 265K. At 15K, the peak around 1.5μm is observed, which is believed to originate from the QDs, while the peak from MQW structure is positioned around 1.4μm. The difference may come from the quantum size effect, i.e., the stacked QDs are confirmed to be thicker than what is targeted due to the limited surface migration inside the cylindrical hole on the SiN_x mask. This is evident from the HR-TEM image in Fig. 5 as the height of the stacked QD is measured to be ~29nm, significantly thicker than the intended thickness. This increased thickness is a result of growth rate enhancement present from the selective area growth. We anticipate that after optimizing the QD thicknesses based on the TEM images, further samples could be fabricated and capped to allow for room temperature PL characterization of the QDs.

Conclusion

Three stacked QD arrays were successfully grown based on (100) InP substrate employing the pattern-transfer technique using BCP. It was found that the optimization on the parameters in PECVD SiN_x and the subsequent RIE are crucial for the reliable selective growth of the stacked QD arrays. TEM images show that the stacked QD arrays were selectively grown on the nano-sized pattern while the stacking fault and twinned plane were observed, which were reported in the context of NW growth in the literature. To overcome these issues, the optimization on the *in-situ* etching using CBr_4 will be necessary to make the surface, before the regrowth, better, removing the line defects, which might be generated during pattern-transfer. Also the use of high index (311)B substrates may be employed to reduce stacking faults, since it has been reported that (311)B substrate can suppress the generation of WZ structure in the NW structure. At low temperature, PL emission, likely from the stacked QD, were observed although obtaining room temperature PL can only be expected after capping the stacked QDs. Also, in order to better control the thickness of the QD within a hole in SiN_x pattern, it will be necessary to more accurately determine the growth rate within the holes in the nano-pattern.

Key findings from this project:

1. We demonstrated an alternate approach to Stranski–Krastanow (SK) QD formation involving the use of nanopatterning with diblock copolymers (DBC) combined with selective MOCVD growth, enabling QD formation over large surface areas intended for device application. This approach allowed for increased control over the QD size and distribution and elimination of the problematic wetting layer associated with SK QDs.
2. Compared with self-assembled QDs, the nanopatterning and selective growth process provides for a greater degree of control over the compositional range within the QDs, allowing for ***tensile-strained***, lattice-matched, or compressively-strained QDs. Tensile-strained (InGaAs) and compressively-strained (InAs) QDs on InP were fabricated and exhibited luminescence near 1.4 and 2.1 microns respectively. We are not aware of any other reports of tensile-strained QDs.
3. The ***first*** nano-patterned QD lasers were fabricated in this program. Lasing was observed only at low temperatures, presumably a result of non-radiative carrier recombination originating from fabrication induced surface states within the QD active region. Additional work is require to reduce non-radiative surface recombination in the QD active region, which is expected to lead to improved performance.
4. In order to further improve the optical properties (i.e. reduce non-radiative recombination) of the QD active region, in-situ etching using CBr_4 prior to the QD deposition showed improved luminescence from the QDs. These techniques need to now be implemented for QD active devices.
5. An optimized DBC process coupled with thicker nitride masking material allowed us to demonstrate ***for the first time*** stacked QDs using the selective growth process. TEM imaging reveals that stacking faults are present in the QDs, similar to that observed in nano-wires fabricated by selective growth epitaxy using a dielectric mask.

References

1. H. Dery, E. Benisty, A. Epstein, R. Alizon, V. Mikhelashvili, G. Eisenstein, R. Schwertberger, D. Gold, J. P. Reithmaier, and A. Forchel, *J. Appl. Phys*., **95**, 6103 (2004).
2. D. R. Matthews, H. D. summers, P. M. Smowton, and M. Hopkinson, *Appl. Phys. Lett.*, **81**, 4904 (2002).
3. R. R. Li, P. D. Dapkus, M. E. Thompson, W. G. Jeong, C. Harrison, P. M. Chaikin, R. A. Register, and D. H. Adamson, *Appl. Phys. Lett.*, **76**, 1689 (2000).
4. J. H. Park, A. A. Khandekar, S. M. Park, L. J. Mawst, T. F. Kuech, P. F. Nealey, *J. Cryst. Growth*, **297**, 283 (2006).
5. J. H. Park, C.-C. Liu, M. K. Rathi, L. J. Mawst, P. F. Nealey, and T. F. Kuech, *J. Nanophoton.*, **3**, 031604 (2009).
6. V C Elarde, A C Bryce, J J Coleman *Electron. Lett.* **41** *1122-1124 2005*
7. J. H. Park , L. J. Mawst, J. Kirch , C.–C. Liu, P. F. Nealey, T. F. Kuech, *Appl. Phys. Lett.* **95**, 113111 2009.
8. Park, Miri, et al. "Block copolymer lithography: periodic arrays of~ 10^{11} holes in 1 square centimeter." *Science* 276.5317 (1997): 1401-1404.
9. R.R. Li, P.D. Dapkus, M.E. Thompson, W.G. Jeong, C. Harrison, P.M. Chaikin, R.A. Register, D.H. Adamson Appl. Phys. Lett., 76 (2000), p. 1689
10. Park, J. H., et al. "Controlled growth of InGaAs/InGaAsP quantum dots on InP substrates employing diblock copolymer lithography." *Applied Physics Letters* 95.11 (2009): 113111-113111.
11. Nuntawong, N., et al. "Effect of strain-compensation in stacked 1.3 μm InAs/GaAs quantum dot active regions grown by metalorganic chemical vapor deposition." *Applied physics letters* 85.15 (2004): 3050-3052.
12. Williams, Kirt R., and Richard S. Muller. "Etch rates for micromachining processing." *Microelectromechanical Systems, Journal of* 5.4 (1996): 256-269.
13. Williams, Kirt R., Kishan Gupta, and Matthew Wasilik. "Etch rates for micromachining processing-Part II." *Microelectromechanical Systems, Journal of* 12.6 (2003): 761-778.
14. Ebert, C., et al. "Selective area etching of InP with CBr4 in MOVPE." *Journal of crystal growth* 298 (2007): 94-97.
15. Mawst, L. J., et al. "Quantum dot active regions based on diblock copolymer nanopatterning and selective MOCVD growth." *Winter Topicals (WTM), 2011 IEEE*. IEEE, 2011.
16. Li, Quan, et al. "Size-Dependent Periodically Twinned ZnSe Nanowires." *Advanced Materials* 16.16 (2004): 1436-1440.
17. Dick, Kimberly A., et al. "Crystal phase engineering in single InAs nanowires." *Nano letters* 10.9 (2010): 3494-3499.
18. Bao, Jiming, et al. "Optical properties of rotationally twinned InP nanowire heterostructures." *Nano letters* 8.3 (2008): 836-841.
19. Shtrikman, Hadas, et al. "Stacking-faults-free zinc blende GaAs nanowires." *Nano letters* 9.1 (2008): 215-219.

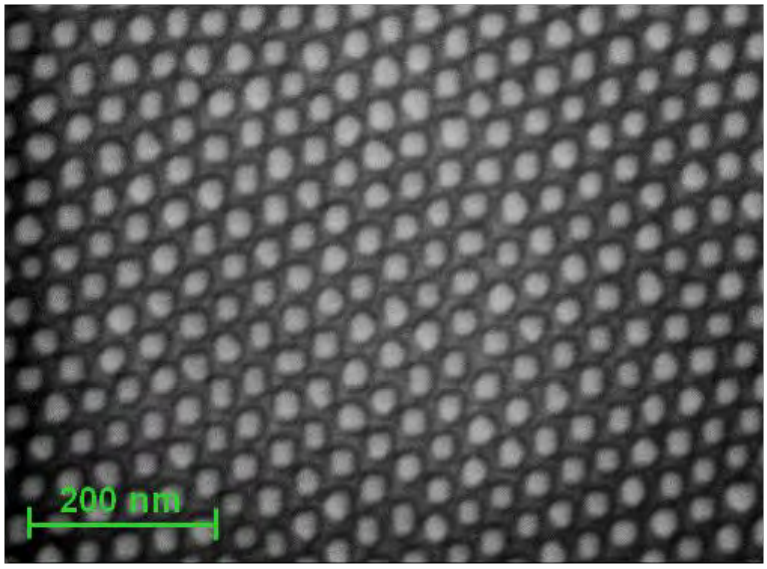

Fig 1. Top view SEM image of InGaAsP(Q1.15)/$In_{0.53}Ga_{0.47}As$/InGaAsP(Q1.15) QDs after selective MOCVD growth.

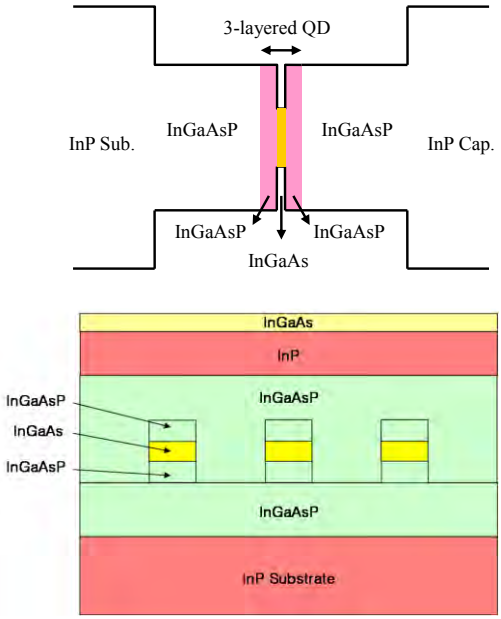

Fig 2. Schematic diagram of QD active laser structure

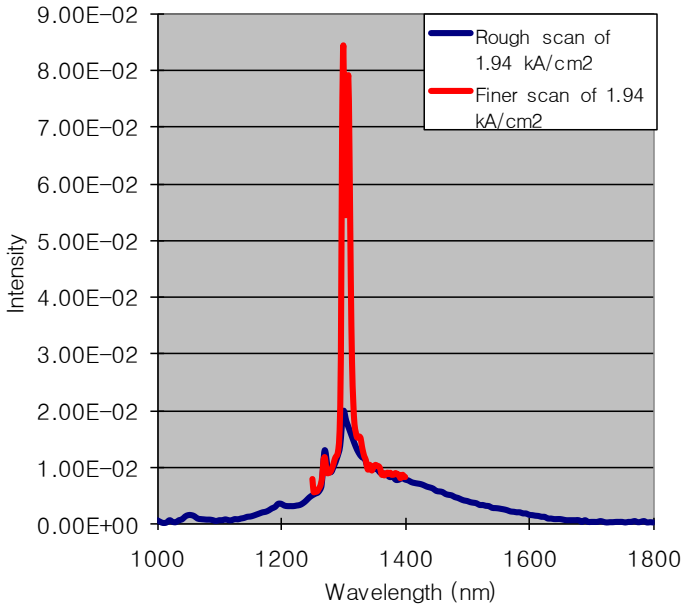

Fig 3. Low temperature, 20K EL spectrum of InGaAsP (Q1.15)/ $In_{0.53}Ga_{0.47}As$/InGaAsP(Q1.15) QD laser with current density of 1.94 KA/cm^2.

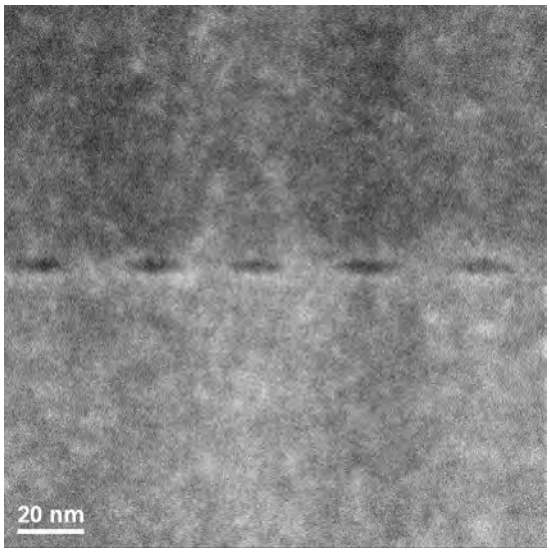

Fig 4. TEM cross-sectional image of the buried QD active region, demonstrating QDs with no wetting layer present.

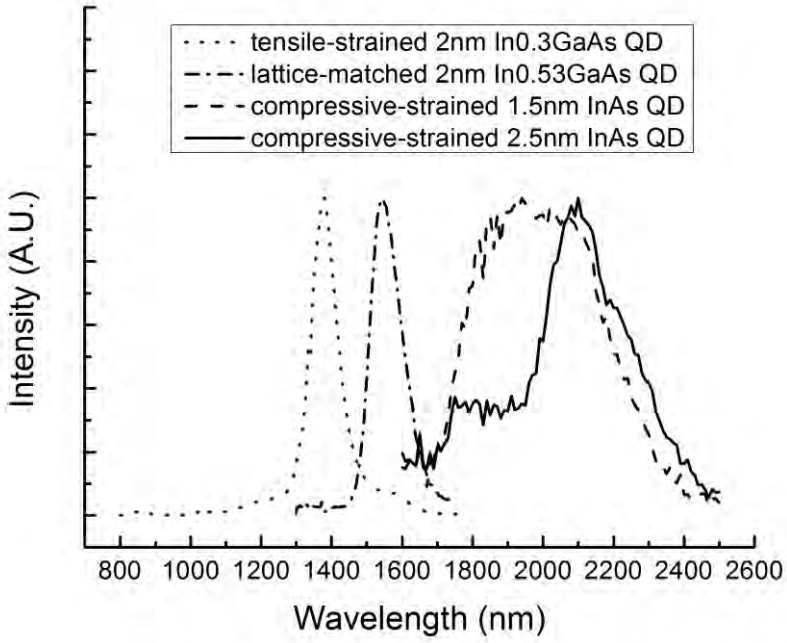

Fig. 5 LT (30K) PL spectrum of tensile-strained, lattice-matched, and compressive-strained In(Ga)As QDs (2nm $In_{0.3}GaAs$ QD, 2nm $In_{0.53}GaAs$ QD, and InAs QDs thicknesses of 1.5nm and 2.5nm). Pre-cleaning procedure (HCL etching) prior to InAs QD growth was employed. PL intensities are normalized.

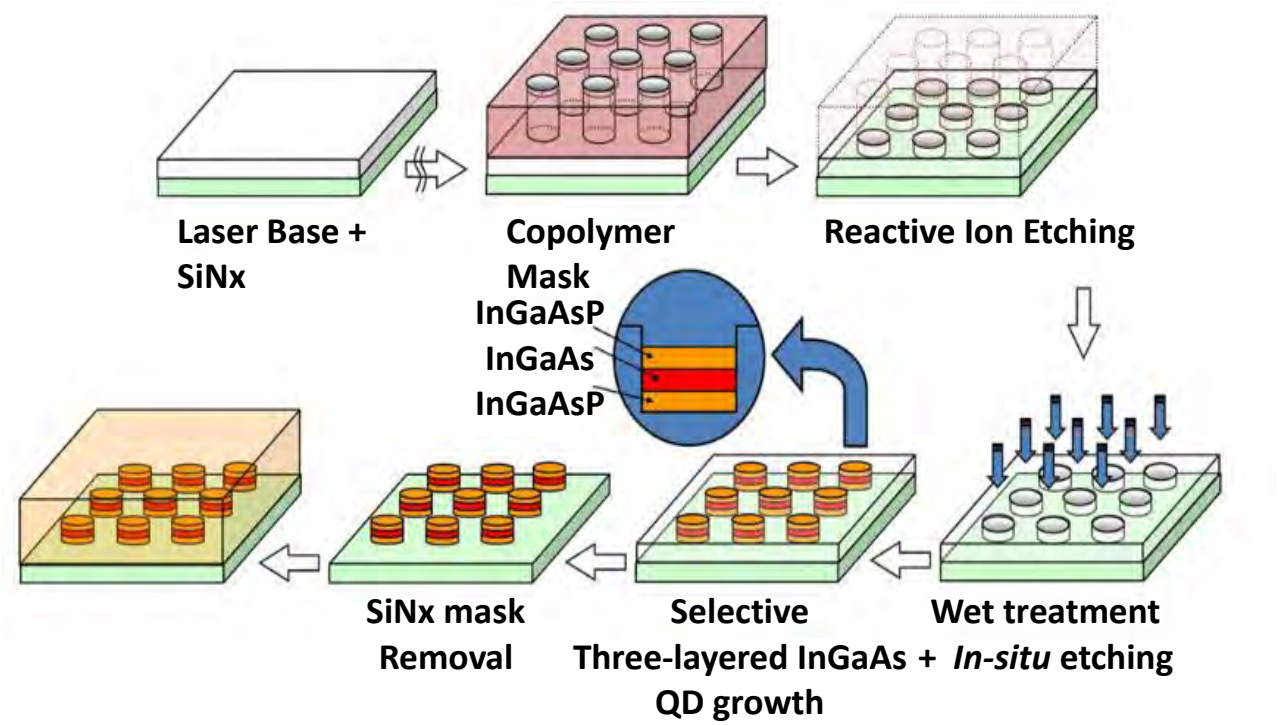

Fig. 6. Selective Growth of QD arrays using Cylinder-forming Diblock Copolymer

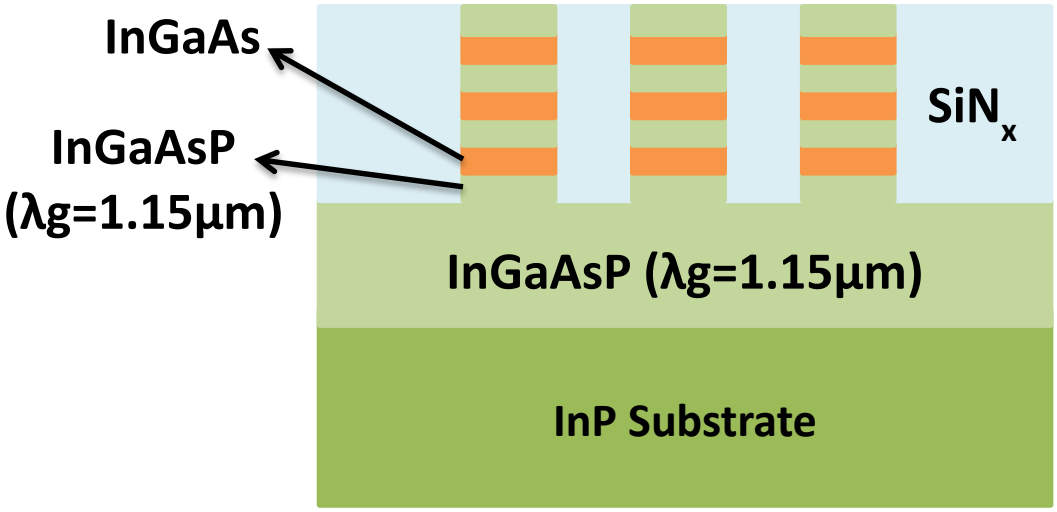

Layers	Thickness	Doping Concentration
3 stack QDs	~14nm	undoped
InGaAsP	150nm	undoped
InP	350µm	5×10^{17}

Fig 7. Laser Base Structure with three stack QD array

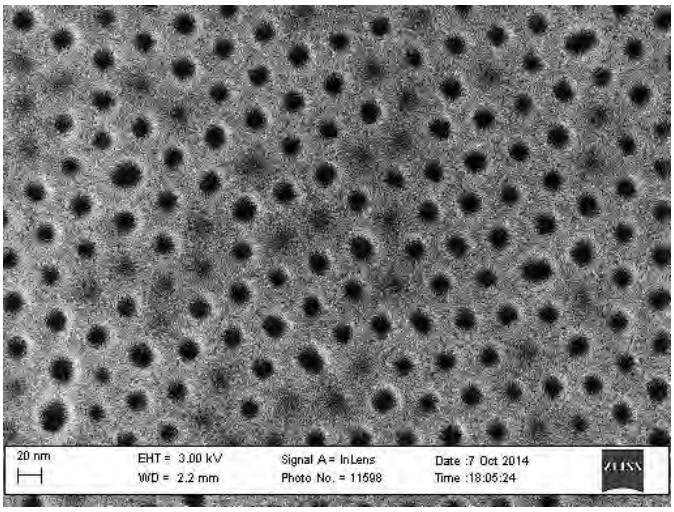

(a) BCP Template

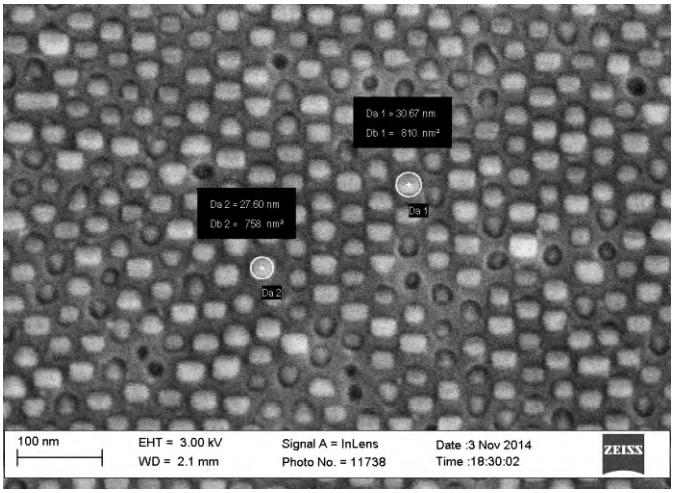

(b) Three QD stacks without SiNx mask removal

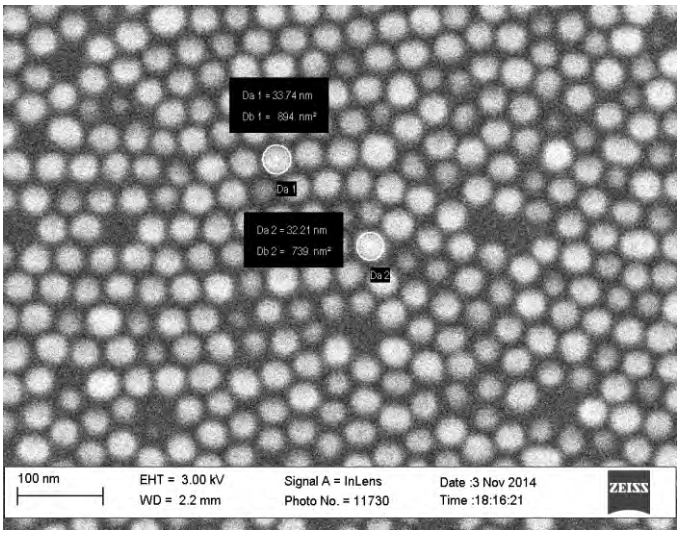

(c) Three QD stacks with SiNx mask removed

Fig. 8 Top view of Scanning Electron Microscopic Images for QDs grown with various RIE time

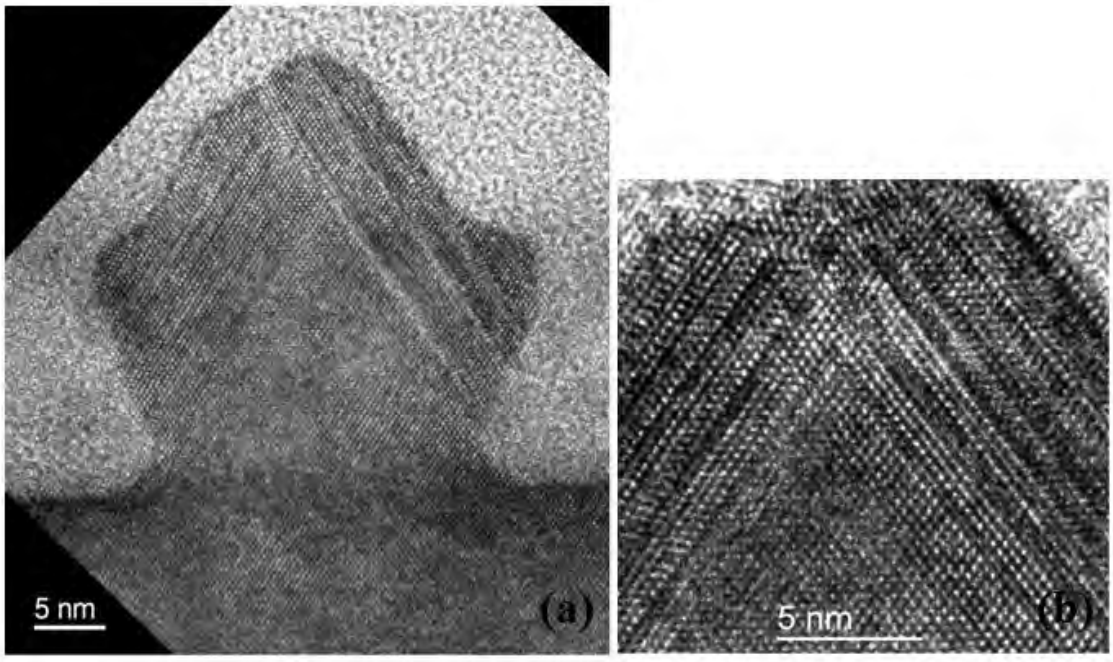

Fig. 9 Cross sectional HR-TEM of a three stacked QD

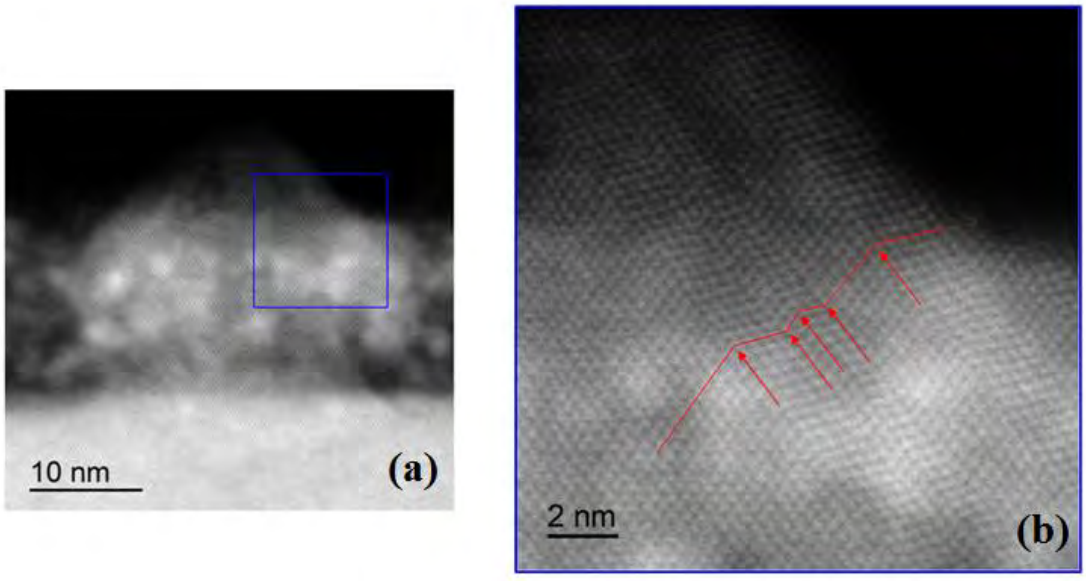

Fig. 10 HR-STEM of a three stacked QD

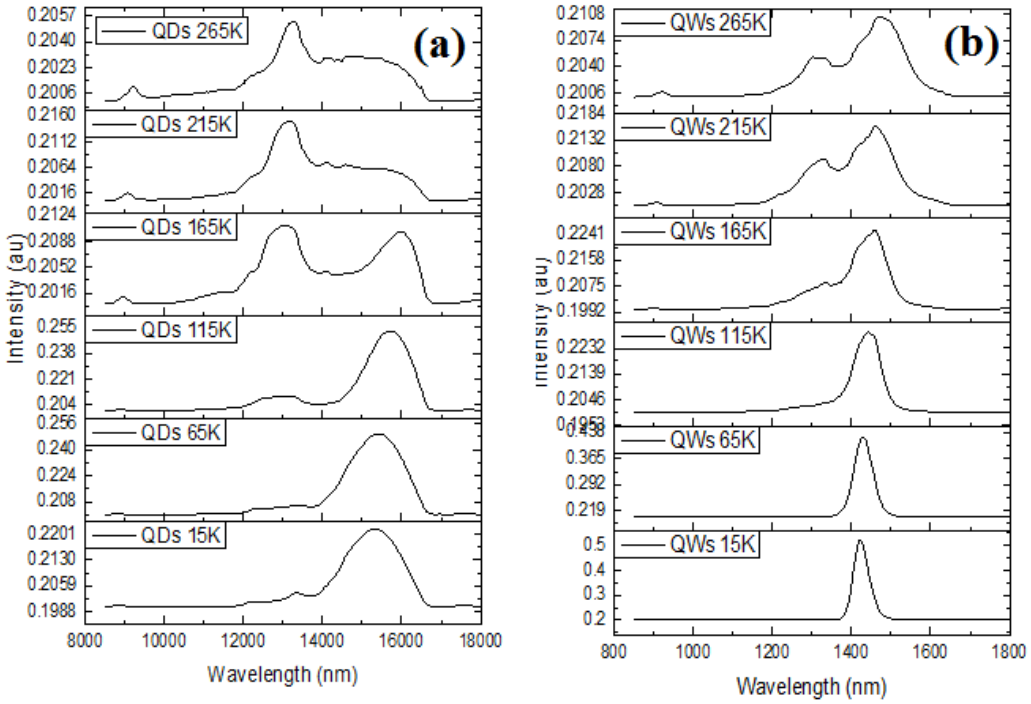

Fig. 11 Temperature dependent PL measurement from (a) three stacked QDs grown with SiNx mask (b) triple QWs grown without SiNx mask on the laser base